Metamorphic evolution of calc-schists in the Central Alps, Switzerland

Barbara K. Kuhn[1],*, Eric Reusser[1], Roger Powell[2] and Detlef Günther[3]

Abstract

Calc-schists of the Mesozoic metasedimentary units in the Central Alps, between the Simplon fault, the Bergell intrusion, the Gotthard massif and the Insubric line, are investigated to assess their metamorphic evolution and to gain a better understanding of scapolite stability and its phase relations. These rocks have only experienced the Mesoalpine metamorphic event. The abundance of silicate minerals in the calc-schists results in a series of characteristic mineral assemblages with increasing metamorphic grade. In the outer part of the Central Alps at lower amphibolite facies conditions, mineral assemblages containing clinozoisite and plagioclase are diagnostic. In areas of intermediate metamorphic grade, clinozoisite and plagioclase are replaced by scapolite-bearing assemblages and K-feldspar begins to form. In the upper amphibolite facies region around Bellinzona clinopyroxene is observed as an additional phase within the scapolite-bearing assemblages. The evolution of mineral assemblages observed from the outer to the central part of the Central Alps can also be identified within individual higher grade rocks. Phase diagram calculations show a good agreement with the observed mineral assemblages and their evolution, helping to validate the new thermodynamic model for scapolite that was used. They allow estimation of the temperature of peak metamorphism. However, the thermodynamic modelling leads to the conclusion that such carbonate-bearing rocks are not well suited to constrain the pressure of metamorphism.

Keywords: Central Alps, calc-schist, scapolite, metamorphic evolution, characteristic mineral assemblages.

1. Introduction

In the Central Alps, between the Simplon fault zone in the West and the Bergell intrusion in the East, most rocks are polymetamorphic except for the Mesozoic sediment cover which has only undergone the Alpine metamorphism. These Mesozoic rocks are lithologically and chemically very heterogeneous (Burckhardt, 1942; Frey, 1974; Günthert, 1954; Kuhn, 2005; Niggli et al., 1936; Trommsdorff, 1966). Varying input of terrestrial detritus into a carbonate depositional environment led to the formation of rocks ranging from pure calcitic or dolomitic marbles to calc-schists and pelitic rocks. In the northern part, south of the Gotthard massif, the Mesozoic metasediments form thick sequences. Towards the South, the Mesozoic metasediments become thinner until they occur as isolated boudins just north of the Insubric line (Fig. 1). Additionally, it is observed that siliceous dolomites are concentrated in the Northern part whereas calc-schists are more widely distributed.

The metamorphic evolution of siliceous dolomites (Trommsdorff, 1966) and metapelitic rocks (Fox, 1975; Frey, 1974; Klaper, 1986; Klaper and Bucher-Nurminen, 1987; Niggli and Niggli, 1965) has been thoroughly studied. The mineral assemblages of calc-schists (known as „Bündnerschiefer" in the Alps) have been described by several authors (Bianconi, 1971; Frey, 1974; Klaper, 1986). However, only few studies focussed on the outer part of the Central Alps have been carried out on their metamorphic evolution (Frank, 1983; Klaper, 1982). Calc-schists are abundant over a wide range of metamorphic conditions, showing a variety of silicate phases suggesting a succession of characteristic mineral assemblages. This offers the opportunity to use the calc-schists to constrain the metamorphic evolution by phase equilibrium calculations. Until now, using these rocks for such a purpose was very difficult due to the lack of a suitable thermodynamic model for scapolite, a key mineral in the calc-schists. Various authors proposed models for scapolite (e.g. Baker and Newton, 1994; Goldsmith and Newton, 1977; Moecher

[1] Institut für Mineralogie und Petrographie, ETH Zürich, 8092 Zürich, Switzerland. <barbara.kuhn@alumni.ethz.ch>
* Present address: Bettlistrasse 5, 8600 Dübendorf, Switzerland.
[2] School of Earth Sciences, University of Melbourne, Victoria 3010, Australia.
[3] Laboratorium für anorganische Chemie, ETH Zürich, 8093 Zürich, Switzerland.
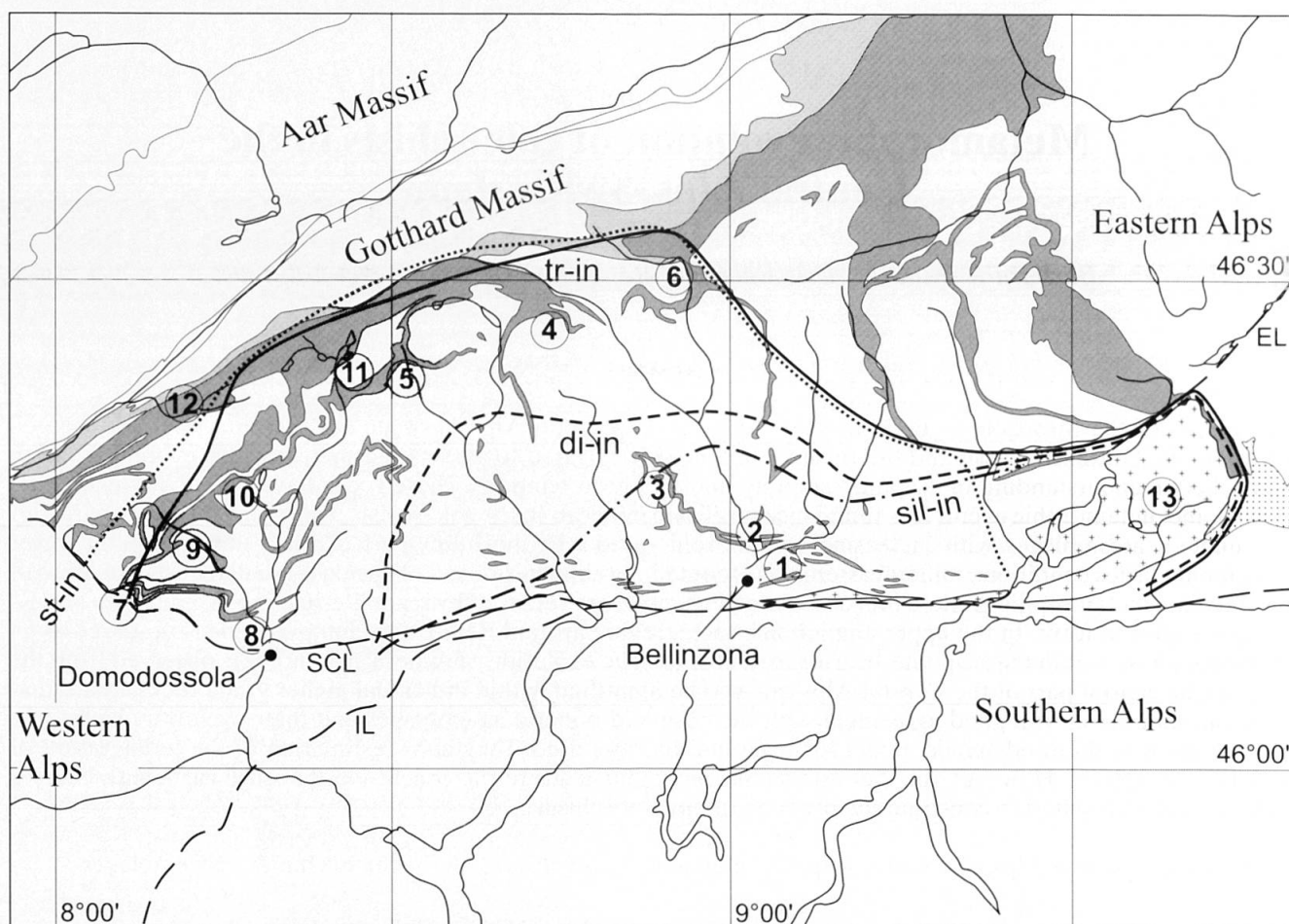
Fig. 1 Schematic map of the Central Alps showing the distribution of carbonate rocks (grey) and the Bergell intrusion (cross pattern). The carbonate occurrences in dark grey belong to the Penninic area while the para-autochthonous sediments of the Gotthard massif are marked in light grey. The formation of staurolite (*st-in*, after Niggli and Niggli, 1965) and of tremolite (*tr-in*, after Trommsdorff, 1966) shows the transition from greenschist facies to lower amphibolite-facies conditions in metapelites and siliceous dolomite marbles, respectively. The formation of diopside or forsterite in the dolomite marbles (*di-in*, after Trommsdorff, 1966) and the occurrence of sillimanite (*sil-in*, after Niggli and Niggli, 1965) in the metapelites indicate upper amphibolite-facies conditions. The areas sampled are numbered as follows. 1: Gesero, 2: Castione, 3: Cima Lunga, 4: Campolungo, 5: Valle Maggia, 6: Val Blenio, 7: Simplon-Zwischbergen, 8: Crèvola d'Ossola, 9: Val Cairasca, 10: Alpe Dèvero, 11: Val Formazza, 12: Binntal, 13: Bergell. IL: Insubric line, SCL: Simplon-Centovalli line, EL: Engadine line. After the Geological map of Switzerland (1980).

and Essene, 1990; Oterdoom and Gunter, 1983). However these models are not appropriate for phase equilibrium calculations as they are not able to predict the stability of scapolite of mizzonitic composition. Here, with a new scapolite model (Kuhn and Powell, in prep.), we investigate the metamorphic evolution of these Alpine calcschists.

2. Geological setting

Studies on mineral zones and mineral assemblages in the Central Alps show a general increase in the metamorphic grade of Alpine metamorphism from the outer to the central part (Fig. 1). The isograds display a more or less concentric shape (Frey et al., 1974; Niggli, 1960; Todd and Essene, 1990; Oterdoom and Gunter, 1983).

Engi, 1997; Trommsdorff, 1966; Trommsdorff, 1990; Wenk, 1970).

In the outer part (e.g. South of the Gotthard massif) the transition from greenschist- to lower amphibolite-facies conditions is characterised by the appearance of tremolite within the dolomite marbles (Trommsdorff, 1966; *tr-in* in Fig. 1) and the change from chloritoid-bearing to staurolite-bearing assemblages in the adjacent metapelites (Fox, 1975; Frey, 1974; Klaper, 1986; Niggli and Niggli, 1965; *st-in* in Fig. 1). Towards the central part the metamorphic conditions increase to upper amphibolite-facies conditions shown by the occurrence of diopside in the dolomite marbles (Trommsdorff, 1966; *di-in* in Fig. 1). In the area around Bellinzona the maximum conditions were reached with sillimanite present in the metapelitic

Table 1 Mineral abbreviations used.

bi	biotite	grt	garnet	pli	anorthitic plagioclase
cc	calcite	hbl	hornblende	q	quartz
chl	chlorite	ksp	K-feldspar	sc	scapolite
cpx	clinopyroxene	ky	kyanite	sil	sillimanite
cz	clinozoisite	mu	muscovite	st	staurolite
di	diopside	pl	plagioclase	tr	tremolite
dol	dolomite	plc	albitic plagioclase	wo	wollastonite

Table 2 Overview on the sampling areas and their geologic context. The numbers correspond to numbers used in Figure 1. In general several calc-schist samples were taken from different localities within the indicated area. In areas marked by * only one sample was taken from one locality. For sample list and exact coordinates see Kuhn (2005).

Sampling area		Geologic and tectonic context
1	Gesero	Bellinzona-Dascio Zone, Southern steep belt
2	Castione	between Simano and Adula nappe
3	Cima Lunga	between Simano nappe and Cima Lunga unit
4	Campolungo	between Leventina and Simano nappe
5	Valle Maggia	between Antigorio and Lebendun / Maggia nappe
6	Val Blenio	between Lucomgagno and Simano nappe
7	Zwischbergen	between Antigorio and Lebendun & between Lebendun and Monte Leone nappe
8	Crèvola d'Ossola*	between Antigorio and Lebendun & between Lebendun and Monte Leone nappe
9	Val Cairasca	below Antigorio and between Antigorio and Lebendun nappe
10	Alpe Dèvero	between Antigorio and Lebendun & between Lebendun and Monte Leone nappe
11	Val Formazza	between Antigorio and Lebendun & above Lebendun nappe
12	Binntal	above Monte Leone nappe
13	Bergell*	Masino window: Gruf unit?

gneisses (Knoblauch and Reinhard, 1939; Niggli and Niggli, 1965; *sil-in* in Fig. 1) and with partial anatexis of the gneisses (Blattner, 1965; Burri et al., 2005).

The sampled areas are shown in Fig. 1 and described in Table 2. Comparing their distribution with the distribution of the isograds shows that a wide range of metamorphic conditions was investigated.

3. Petrography

3.1. Macroscopic description

Calc-schists are characterised by the abundant occurrence of white boudins and layers of different sizes oriented parallel to the schistosity and consisting of quartz or calcite. Their protoliths are mixtures of calcareous and pelitic sediments in variable proportions yielding rocks which are heterogeneous in composition as well as in grain size. Consequently, modal proportions of minerals vary over short distances. In most outcrops, the calc-schists are fine-grained and strongly foliated. Silicate phases are often concentrated in layers alternating with calcite-rich layers. Biotite and muscovite define the schistosity. Most minerals (e.g. calcite, quartz, biotite, muscovite) are fine-grained, but garnet, plagioclase and scapolite can
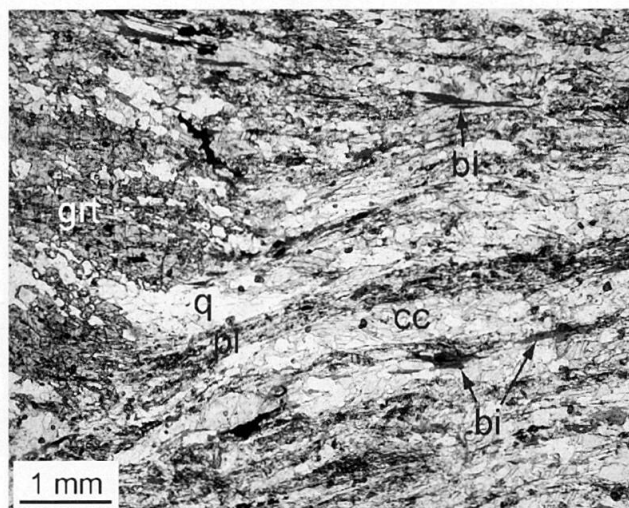
Fig. 2 Thin section of calc-schists: general view. Val Formazza, sample Atg65. Plane-polarised light.

form coarse (up to 1cm size) grains. Rocks from the areas in the most central area, Gesero (E of Bellinzona) and Castione (N of Bellinzona), are coarse-grained and appear massive in hand sample, although a pronounced schistosity is observed in the outcrops.

3.2. Microscopic description

A typical texture of the calc-schists is shown in Fig. 2. Calcite is commonly elongated parallel to
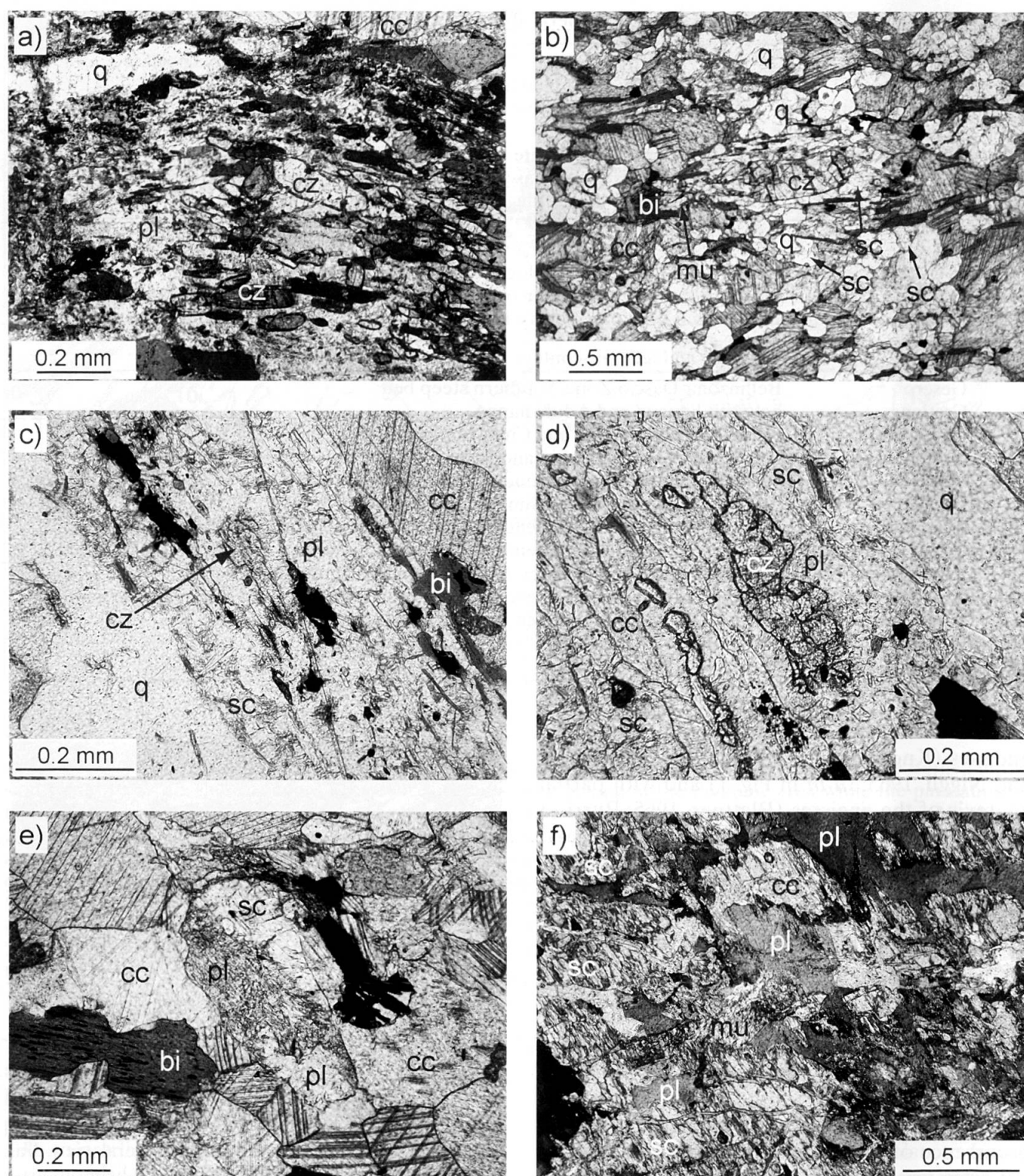
Fig. 3 Photomicrographs: (a) Clinozoisite is often included in plagioclase. Sample Cmp20; Campolungo. Crossed polarisers. (b) Scapolite overgrowing clinozoisite. Cima Lunga, sample CL76. Plane-polarised light. (c) and (d) Clinozoisite overgrown by plagioclase which is later reacting to scapolite. Crèvola d'Ossola, sample Atg61. Both in plane-polarised light. (e) Scapolite forming from or decomposing to plagioclase. No criteria indicate the direction of the reaction. Gesero, sample Ges27. Plane-polarised light. (f) Scapolite decomposing to plagioclase and calcite. Cima Lunga, sample CL78. Crossed polarisers.

the foliation whereas quartz is rounded. Biotite and muscovite define the foliation. Clinozoisite occurs as more or less isometric grains or as prisms, which are oriented parallel to the folia-

tion. In general they are small but can also be up to half a millimetre long. Clinozoisite is often included in plagioclase (Fig. 3a) and also in garnet or scapolite (Fig. 3b and 4a). Plagioclase is abun-

Fig. 4 Backscattered electron (BSE) images of scapolite textures. (a) Clinozoisite overgrown by scapolite. Cima Lunga, sample CL76. (b) Clinozoisite overgrow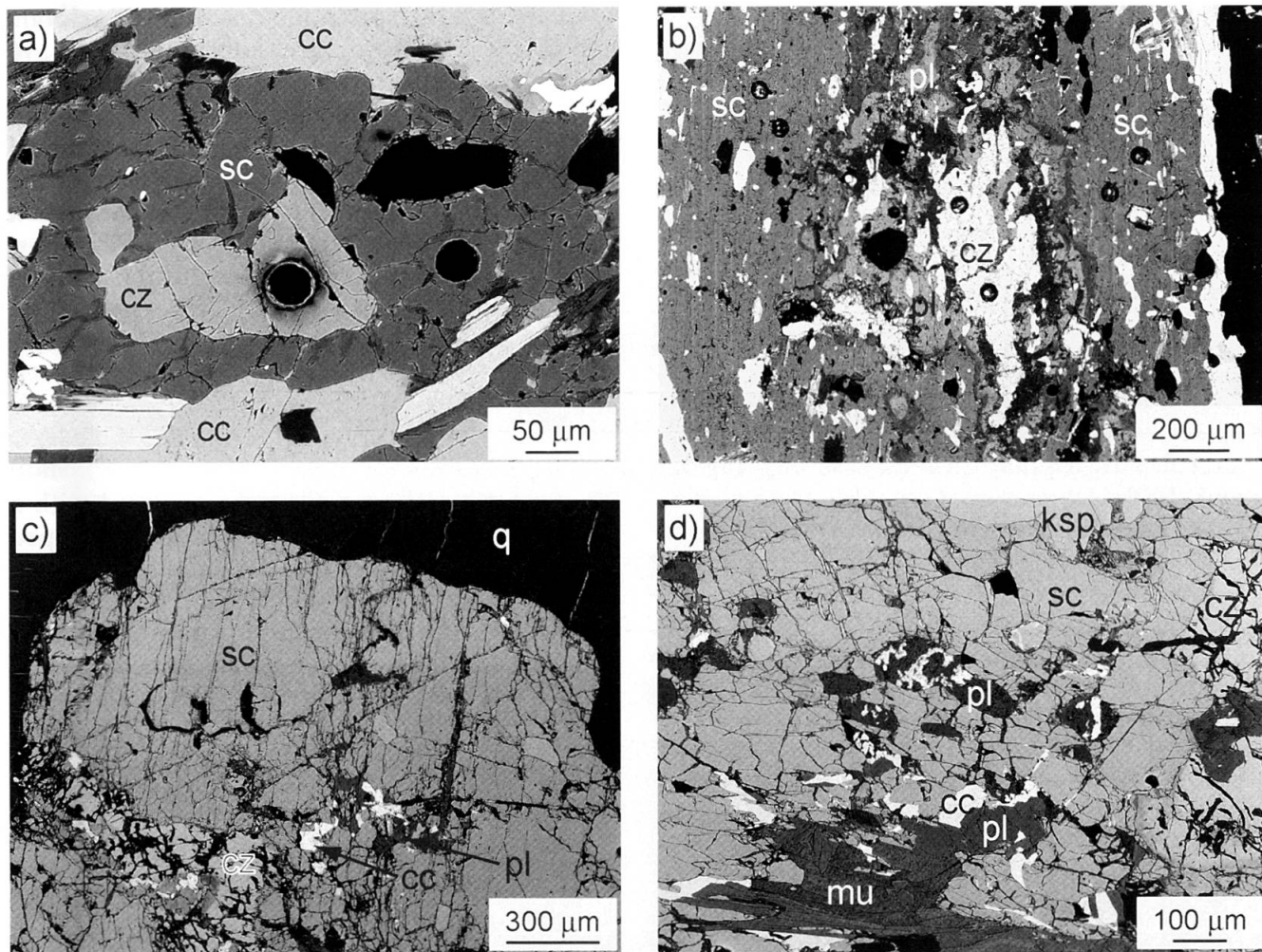n by plagioclase which is later reacting to scapolite. Crèvola d'Ossola, sample Atg61. The black holes in a and b are laser ablation pits. (c) Idiomorphic scapolite crystal decomposing to plagioclase and calcite along cracks. Castione, sample Cst83.2. (d) Plagioclase and calcite forming from scapolite inside a big scapolite crystal. Castione, sample Cst83.1.

dant and grows mostly as large poikiloblastic crystals (up to 6 mm) rich in inclusions. Some plagioclase crystals are zoned. Garnet is always larger (up to 5 mm in diameter) than the other minerals but is not present in all samples. It is scarcely idiomorphic but helicitic or broken with many inclusions (Fig. 2) and sometimes even elongated. Diopside is rare and is only present in samples from Castione or Gesero. It forms 4–5 mm large crystals, which are commonly broken or helicitic. Amphiboles are even rarer and then mostly overgrow diopside. They have a green colour with a blue-green pleochroism which suggests a hornblende composition. Scapolite occurs in samples from the middle and the central part and may be found in modal amounts of up to 40%. It can be small and round or elongated. Sometimes it forms almost idiomorphic crystals which are up to 8 mm long, but it also grows poikiloblastically incorporating biotite and/or quartz. Ragged grain boundaries between scapolite and plagioclase can be observed.

Pyrite, titanite, rutile, graphite and tourmaline are the common accessory minerals. Typically, titanite occurs as small idiomorphic crystals which sometimes include rutile. Graphite occurs as a very fine-grained black mass. In samples from Gesero, Castione and Cima Lunga, graphite forms small platelets. Idiomorphic crystals of tourmaline are tiny and green.

3.3. Textures and reactions

Although in general the textures do not reflect reaction, suggesting the effective operation of progressive over-printing of mineral assemblages, in rare cases, reaction textures can be observed. Over the whole area investigated, clinozoisite is usually included in plagioclase (Fig. 3a). In the areas where scapolite is present, its formation is observed from plagioclase (Fig. 3c, d) or directly from clinozoisite (Fig. 3b and 4a). Figs. 3c, d and 4b show that alternatively clinozoisite can also be

Table 3 Definition of the scapolite components.

meionite	$Ca_3Al_6Si_6O_{24} \cdot CaCO_3$
marialite	$Na_3Al_3Si_9O_{24} \cdot NaCl$
sylvialite	$Ca_3Al_6Si_6O_{24} \cdot CaSO_4$
mizzonite	$NaCa_2Al_5Si_7O_{24} \cdot CaCO_3$
CO_3-marialite*	$Na_3Al_3Si_9O_{24} \cdot CaCO_3$

* CO_3-marialite is a hypothetical end-member used to set up the thermodynamic activity-composition model of scapolite.

overgrown in two steps. First clinozoisite reacts to plagioclase. In a second step plagioclase becomes overgrown by scapolite. In a few cases (e.g. Fig. 3c, d and 4b) the formation of scapolite from plagioclase is obvious. However, in most thin sections (e.g. Fig. 3e) the direction of reaction progress cannot be deduced from the reaction textures.

In calc-schist samples from the Cima Lunga and Castione large almost idiomorphic scapolite crystals are decomposing to plagioclase and calcite (Fig. 3f, 4c and d). Although the formation of scapolite from plagioclase and calcite is common-

ly thought to be a prograde reaction (Oterdoom, 1980), these textures are interpreted to have formed during the retrograde history. Another indication of retrograde reactions is the development of colourless edges, rims and lamellae of chlorite in biotite (Fig. 5a) that occur all over the Central Alps. In a few samples the chloritisation of garnet is also observed (Fig. 5b). In the most central areas clinopyroxene can be replaced by amphibole (Fig. 5c).

4. Mineral compositions

4.1. Analytical methods

The mineral compositions were analysed with a Cameca SX50 electron microprobe equipped with 5 WD spectrometers. Typical measurement conditions were 15 kV acceleration potential, 20 nA probe current, 20 s acquisition time on peak (10 s on background positions) for all elements except Cl and S for which 40 s were used. The standards used were natural and synthetic silicate compounds (for a list of standards see Kuhn, 2005). The
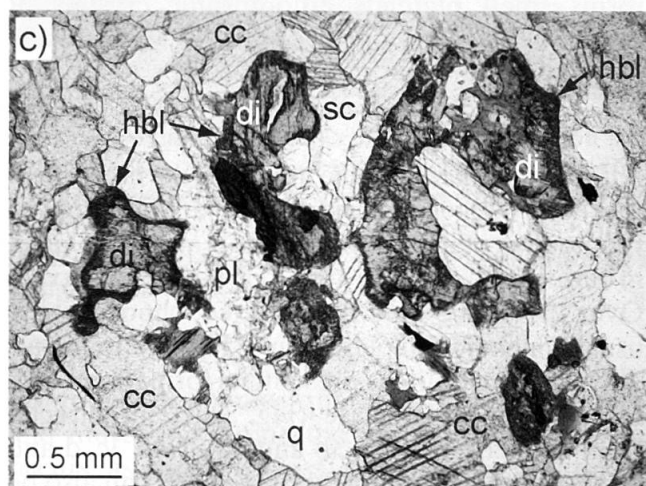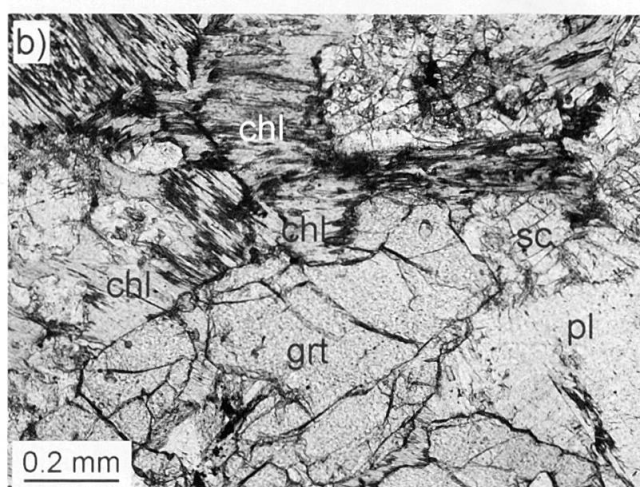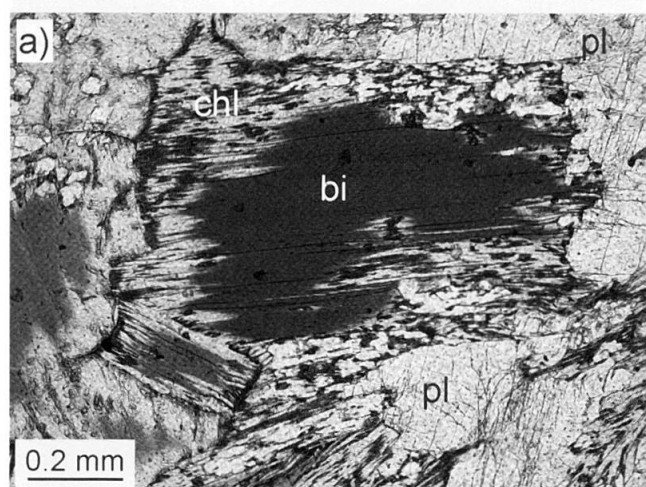
Fig. 5 Photomicrographs showing retrograde reactions: (a) Biotite decomposes to chlorite. (b) Garnet decomposes to chlorite. Both reactions are observed in sample Cst5c from Castione. (c) A retrograde amphibole rim on clinopyroxene. Gesero, sample Ges26. All in plane-polarised light.

recalculations of the analyses to the mineral formulae were performed by using code written by the authors (for the exact procedure, see Table 4).

4.2. Results

Clinozoisite shows two different compositions within the same rocks: an almost pure Al-end-member, $X_{Ep} = Fe^{3+} / (Fe^{3+} + Al - 2) = 0–0.1$, and a Fe^{3+}-bearing variety with $X_{Ep} = 0.2–0.4$. Both varieties occur as inclusions in plagioclase and scapolite with the Fe-rich grains being tiny whereas the almost pure clinozoisite forms relatively large crystals. Plagioclase has a wide range of compositions ($X_{An} = 0.15–1$) showing three maxima at $X_{An} = 0.25–0.4$, $0.6–0.75$ and $0.85–1$ (Fig. 6). It is commonly zoned with irregularly shaped Na-rich rims. Sometimes a two step enrichment in Na can be observed towards the grain boundary with scapolite (Fig. 7). Scapolite forms a solid solution between meionite and marialite (see Table 3) which may also incorporate SO_4 on the anion site. In calc-schists, scapolites have a rather meionite-rich composition with an equivalent anorthite content $X_{eqan} = (Al - 3) / 3$ (Ellis, 1978) between 0.62 and 0.82. The special anion site is dominated by CO_3 with very little Cl or SO_4.

Clinopyroxenes from Castione and Gesero are Mg-rich, with $Mg / (Mg + Fe) = 0.5–0.88$. Garnet is primarily a mixture of almandine and gros-

Table 4 Representative mineral compositions of scapolite, plagioclase, garnet and clinopyroxene. Scapolite and plagioclase marked by a), b) etc. are from coexisting pairs. Selected mineral analyses.
** CO_2 is calculated from the stoichiometry of scapolite. * FeO and Fe_2O_3 are recalculated from the charge balance.

Scapolite [recalculated to Al + Si = 12]						
Sample	CL78_5 a)	CL78_8 b)	CL78_18 c)	Atg61_72 d)	Atg61_106 e)	Atg61_145 f)
SiO_2	45.72	45.53	45.99	45.3	45.12	46.64
Al_2O_3	28.66	28.89	27.39	28.9	28.84	27.52
FeO	0.09	0.08	0.07	0.09	0.08	< 0.04
CaO	18.47	18.69	18.07	18.6	19.03	17.91
Na_2O	2.92	2.9	3.24	3.02	2.94	3.43
K_2O	0.12	0.1	0.14	0.09	0.08	0.08
Cl	< 0.01	< 0.01	< 0.01	< 0.01	< 0.01	0.06
SO_3	< 0.01	< 0.01	< 0.01	< 0.01	< 0.01	< 0.01
CO_2**	4.8	4.81	4.75	4.81	4.81	4.73
Total	100.79	101.01	99.66	100.82	100.92	100.4
Endmembers:						
Meionite	0.78	0.78	0.76	0.77	0.78	0.74
Marialite	0.22	0.22	0.24	0.23	0.22	0.26
$X_{eqan} = (Al-3)/3$	0.71	0.72	0.65	0.72	0.72	0.65

Garnet [recalculated to 8 cations and 12 oxygen atoms]						
Sample	Cst2_m2	Cmp92_m9a	Ges30_m29	Atg64_m7	Wal102_m13	Mag144_m21
SiO_2	37.5	37.39	37.95	37.48	37.49	36.83
TiO_2	0.05	0.09	0.07	0.08	0.12	0.08
Al_2O_3	22.15	21.12	21.44	21.68	21.74	21.33
Cr_2O_3	< 0.03	< 0.03	0.05	< 0.03	< 0.03	< 0.03
Fe_2O_3*	2.38	0.54	1.15	0	0	0.8
FeO*	21.22	28.51	20.22	27.3	27.63	27.47
MnO	1.34	1.05	1.93	1.47	2.58	2.37
MgO	1.92	2.6	1.39	2.54	2.15	1.91
CaO	14.75	8.25	16.17	8.82	7.98	8.36
Na_2O	< 0.04	< 0.04	< 0.04	< 0.04	< 0.04	< 0.04
K_2O	< 0.02	< 0.02	< 0.02	< 0.02	< 0.02	< 0.02
Total	101.34	99.58	100.39	99.38	99.71	99.21
Endmembers						
Grossular	0.35	0.22	0.42	0.25	0.23	0.22
Almandine	0.47	0.64	0.45	0.61	0.62	0.62
Pyrope	0.08	0.10	0.06	0.10	0.09	0.08
Spessartite	0.03	0.02	0.04	0.03	0.06	0.06
Andradite	0.07	0.02	0.03	0.00	0.00	0.03
Uvarovite	0.00	0.00	0.00	0.00	0.00	0.00

(continued)

sular with little pyrope component ($\leq 10\%$). The garnets from Gesero and Castione are richer in grossular (Ca / (Ca + Mg + Fe + Mn) = 0.26–0.45) than the ones from other areas (Ca / (Ca + Mg + Fe + Mn) = 0.21–0.25). Biotite contains normally more Mg than Fe^{2+}. The content of octahedrally coordinated Al is ≤ 0.2 p.f.u.

The composition ranges of most minerals are wide because of the heterogeneity of bulk composition of the calc-schists. Thus, it is difficult to identify trends in mineral composition with metamorphic grade. Representative mineral analyses are reported in Table 4.

4.3. Composition of scapolite-plagioclase pairs

Figure 6 summarises the composition relationship of adjacent scapolite-plagioclase pairs. In general, the variation of scapolite composition is constrained to a narrow range ($X_{eqan} = 0.62$–0.82) whereas

plagioclase shows a wide compositional range ($X_{An} = 0.25$–1).

At Cima Lunga (samples CL76, 78; Fig. 6a) three distinct ranges of plagioclase compositions are observed: (1) albitic plagioclase ($X_{An} = 0.25$–0.42) coexisting with relatively Na-rich scapolite ($X_{eqan} = 0.64$–0.70); (2) intermediate plagioclase ($X_{An} = 0.57$–0.70); and (3) anorthite-rich plagioclase ($X_{An} = 0.87$–0.90) coexisting with meionite-rich scapolite ($X_{eqan} = 0.70$–0.74). Clear compositional gaps are seen between the plagioclase groups.

At Crèvola d'Ossola (sample Atg61; Fig. 6b) the distribution of compositions between scapolite–plagioclase pairs is nearly the same as the one at Cima Lunga, but the gaps between the plagioclase compositional ranges are not well defined. The variation is confined to $X_{eqan} = 0.64$ to 0.74, whereas the plagioclase composition ranges from $X_{An} = 0.28$ to $X_{An} = 0.93$.

Table 4 (continued).

Plagioclase [recalculated to 5 cations]

Sample	CL78_7 a)	CL78_9 b)	CL78_19 c)	Atg61_71 d)	Atg61_107 e)	Atg61_146 f)
SiO_2	46.28	52.16	60.54	44.68	50.83	61.12
Al_2O_3	34.89	31.42	24.92	35.75	31.45	25.13
FeO	0.05	< 0.04	0.05	< 0.04	0.06	< 0.04
CaO	17.57	13.38	6.08	18.57	13.94	6.21
Na_2O	1.48	3.92	8.08	0.96	4.01	8.13
K_2O	0.03	0.08	0.13	0.02	0.04	0.14
Cl	< 0.01	< 0.01	< 0.01	< 0.01	< 0.01	< 0.01
SO_3	< 0.01	< 0.01	< 0.01	< 0.01	< 0.01	< 0.01
Total	100.32	101.01	99.81	100.01	100.33	100.76
Endmembers:						
Orthoclase	0	0	0.01	0	0	0.01
Albite	0.13	0.34	0.7	0.09	0.34	0.7
Anorthite	0.87	0.65	0.29	0.91	0.66	0.29
$X_{An} = Ca/(Ca+Na+K)$	0.87	0.65	0.29	0.91	0.66	0.3

Clinopyroxene [recalculated to 4 cations and 6 oxygen atoms]

| Sample	Cst2_m6	Cst3_m2	Ges25_m5	Ges30_m23
SiO_2	51.45	51.69	53.49	50.45
TiO_2	0.04	0.12	0.05	0.09
Al_2O_3	0.66	1.57	0.88	1.32
Cr_2O_3	< 0.03	0.06	< 0.03	< 0.03
Fe_2O_3*	0.79	1.36	0.81	0.79
FeO*	14.73	8.67	4.13	14.56
MnO	0.52	0.16	0.12	0.34
MgO	8.94	11.94	15.11	8.55
CaO	23.29	24.35	24.53	22.9
Na_2O	0.1	0.13	0.3	0.2
K_2O	< 0.02	< 0.02	< 0.02	< 0.02
Total	100.54	100.05	99.43	99.21
Endmembers				
Wollastonite	0.47	0.47	0.48	0.46
Enstatite	0.26	0.34	0.42	0.25
Ferrosilite	0.24	0.14	0.06	0.24
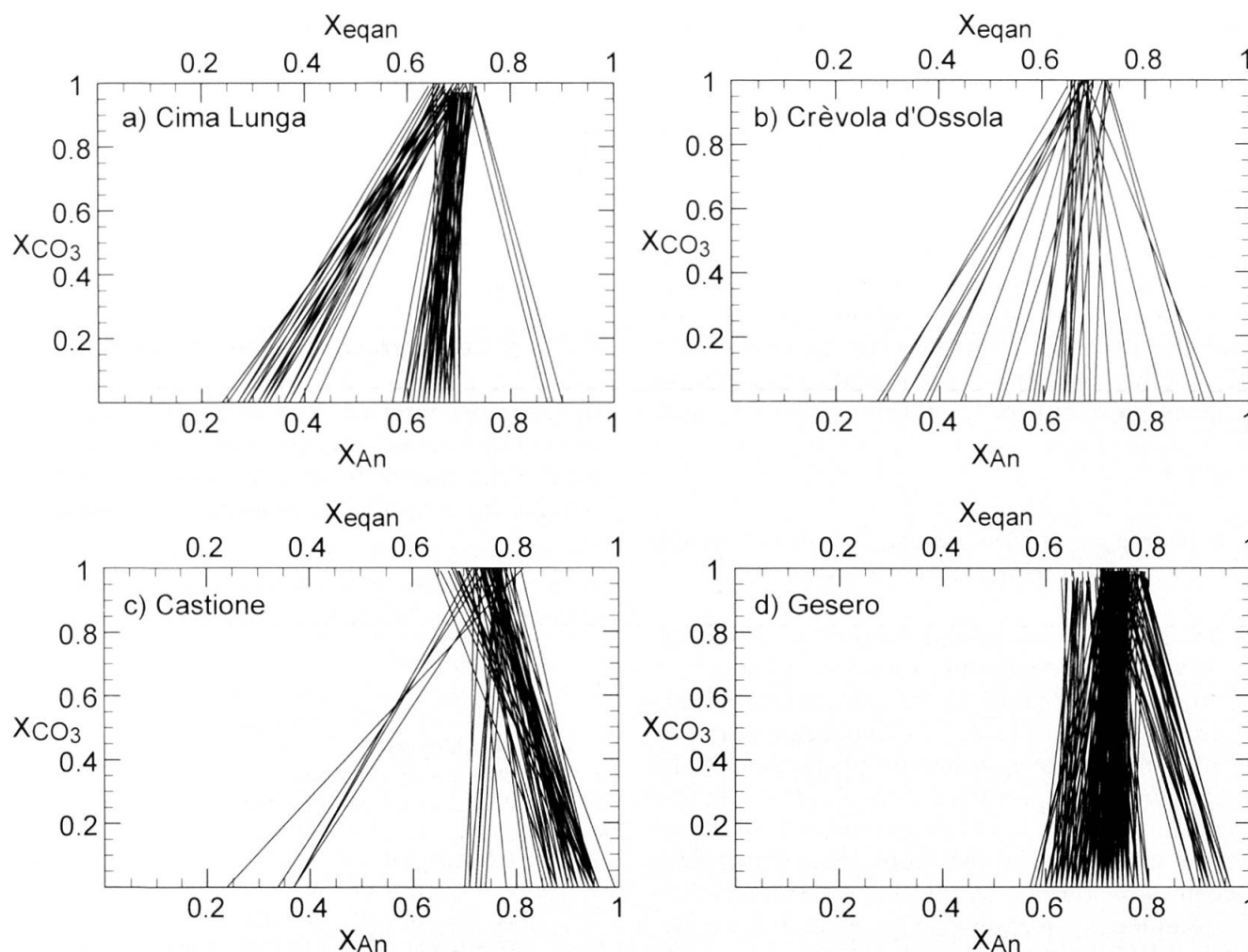
Fig. 6 Composition relations of scapolite-plagioclase pairs from (a) Cima Lunga, (b) Crèvola d'Ossola, (c) Castione and (d) Gesero.

In the central part at Castione (samples Cst2, 3, 5, 83, 84; Fig. 6c) three ranges of plagioclase compositions are observed, but the distinction between the second (X_{An} = 0.70–0.77) and the third (X_{An} = 0.82–1.0) is poorly defined. At Gesero (samples Ges21, 22, 24–27, 30, 31; Fig. 6d) only two plagioclase compositional ranges are seen: (1) intermediate plagioclase (X_{An} = 0.57–0.80) coexisting with relatively Na-rich scapolite (X_{eqan} = 0.63–0.78); and (2) anorthite-rich plagioclase (X_{An} = 0.86–0.96) coexisting with a meionite-rich scapolite (X_{eqan} = 0.70–0.82).

In most samples, the plagioclase-scapolite pairs with the most albitic or anorthitic plagioclase compositions (Cima Lunga, Crèvola d'Ossola and Castione: plagioclase-ranges 1 + 3; Gesero: plagioclase-ranges 1 + 2) clearly coexist with calcite. Similar observations regarding the distributional pattern and the coexistence with calcite were reported by Oterdoom (1979, 1980) from calc-silicate rocks occurring in Val Schiesone.

Details of a grain boundary between scapolite and plagioclase from sample Cst3 (Castione) are shown in Fig. 7. The backscattered electron image and the elemental distribution maps display a zonation pattern with three distinct plagioclase compositions: (1) Most of the plagioclase surrounding scapolite is anorthite-rich; (2) A slightly less Ca-rich plagioclase forms a rim towards scapolite; and (3) The plagioclase proximal to the scapolite has the most albitic composition and coexists with calcite.

5. Observed mineral assemblages and their evolution

From the few observable reactions described in section 3.3, the metamorphic evolution can at least partly be delineated. The stable mineral assemblages at peak metamorphic conditions change with increasing temperature and pressure from the outer part to the central part of the Central Alps. However, the presence of calcite, quartz, biotite and muscovite appears to be unaffected by the changes in temperature and pressure.

5.1 Outer part (Val Blenio, Campolungo, Valle Maggia, Zwischbergen, Val Formazza)

In the external part, the calc-schists are fine-grained. Clinozoisite is commonly included in plagioclase (Fig. 3a). Therefore, we interpret the assemblage calcite, quartz, biotite, muscovite, clinozoisite with sometimes garnet (assemblage #1 in Table 5) to represent the precursor mineral assemblage, whereas calcite, quartz, biotite, muscovite, plagioclase ± garnet (Fig. 8a; assemblage #2 in Table 5) represents the stable assemblage at peak metamorphic conditions. Chlorite is always a late phase formed during the retrograde history.

5.2 Middle part (Cima Lunga, Crèvola d'Ossola, Val Cairasca, Alpe Dèvero)

Scapolite and K-feldspar are observed additionally to calcite, quartz, biotite, muscovite, plagioclase, clinozoisite and garnet in the calc-schists (assemblages #1, #3, #4 in Table 5). Clinozoisite is an early phase overgrown either by plagioclase or by scapolite. In samples from Crèvola d'Ossola and the Cima Lunga unit the overgrowth of clinozoisite takes place in two steps. First, clinozoisite becomes overgrown by plagioclase which is then surrounded by scapolite (Fig. 3c, d, 4b). As described above, scapolite may break down to plagio-

clase and calcite (Fig. 3f). This observation suggests that scapolite is the stable phase at peak metamorphic conditions, whereas plagioclase occurs as a late prograde and retrograde phase. Therefore the stable assemblage in this area is calcite, quartz, biotite, muscovite, scapolite, K-feldspar and garnet (Fig. 8b; assemblage #4 in Table 5). Chlorite forms as a retrograde phase from biotite or garnet.

5.3 Central part (Gesero, Castione)

In the most internal part of the Central Alps, around Bellinzona, clinopyroxene occurs together with calcite, quartz, biotite, muscovite, plagioclase, clinozoisite, scapolite, K-feldspar and sometimes

Table 5 Overview of the observed mineral assemblages in calc-schists. #: Assemblage number.

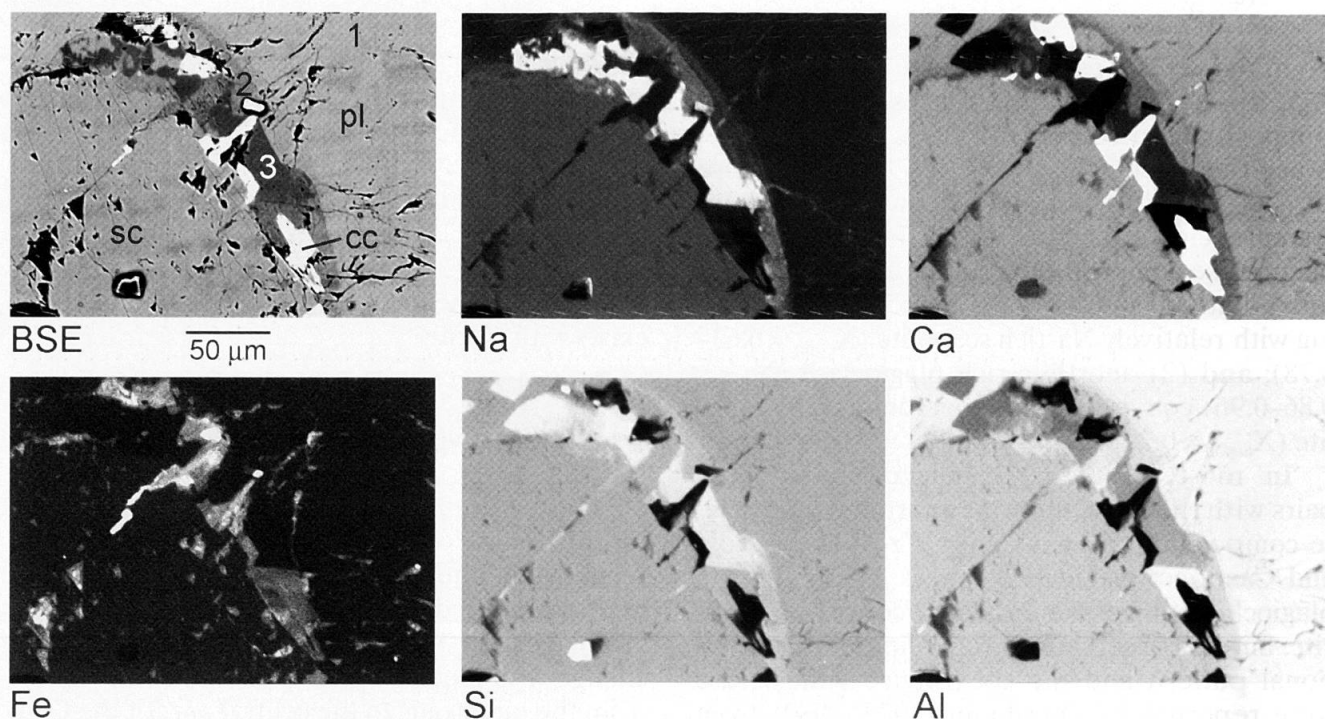| #	
	Outer part
1	cc + q + cz + bi + mu ± grt
2	cc + q + pl + bi + mu ± grt
	Middle part
1	cc + q + cz + bi + mu
3	cc + q + cz + pl + bi + mu
4	cc + q + sc + ksp + bi + mu ± grt
	Central part
3	cc + q + cz + pl + bi + mu
5	cc + q + pl + sc + bi + mu
6	cc + q + sc + ksp + cpx ± bi ± grt

Fig. 7 Backscattered electron (BSE) image and elemental distribution maps of a scapolite-plagioclase boundary in sample Cst3 from Castione. In plagioclase successive Na-enrichment towards the grain boundary with scapolite is observed. 1: $X_{An} = 0.95$, 2: $X_{An} = 0.72$, 3: $X_{An} = 0.24$.

garnet. K-feldspar forms from muscovite break-down at peak metamorphic conditions. The observed textures and reactions suggest that the stable assemblage at peak metamorphic conditions consists of calcite, quartz, biotite, scapolite, K-feldspar, clinopyroxene and garnet (Fig. 8c; assemblage #6 in Table 5). In the retrograde history, minor plagioclase, amphibole and chlorite form.

5.4 Summary of the observed assemblage succession

The succession of observed mineral assemblages in calc-schists is summarised in Table 5. The prograde evolution of the calc-schist is best described by the different assemblages observed to be overgrown and thus preserved in each area. The evolution of mineral assemblages observed from the outer to the central part in the Central Alps can also be identified within individual higher grade rocks of the central part.

6. T–X_{CO2}-equilibria

Phase diagram calculation of the mineral assemblages was done with THERMOCALC 3.22 (Powell et al., 1998) using the internally-consistent dataset of Holland and Powell (1998). For scapolite, a new activity-composition model (Kuhn and Powell, in prep.) describes the mixing between meionite and a hypothetical carbonate-marialite end-member (Table 5) based on the observation that scapolite shows two mixing line segments, one between meionite and mizzonite (Table 3) and the other between mizzonite and marialite. It considers order-disorder of Al and Si on the tetrahedral site so that the intermediate composition mizzonite is stabilised. The new scapolite mixing model allows the modelling of scapolite-bearing assemblages with scapolite compositions comparable to natural ones in a geologically-realistic chemical system.

Calc-schists are well described in the system $Na_2O–CaO–K_2O–FeO–MgO–Al_2O_3–SiO_2–CO_2–H_2O$ with calcite and quartz always present. The average composition of 9 samples representing a typical range of calc-schist compositions (Table 6) was used for the calculation of the T–X_{CO2}-pseudosection at a pressure of 5 kbar (Fig. 9). This pressure is assumed to represent a reasonable value for the outer parts of the Central Alps (Fox, 1975; Frey, 1978). At this pressure, scapolite forms at temperatures as low as 460 °C. In water-rich (low X_{CO2}) environments, assemblages contain clinozoisite and albitic plagioclase. With increasing temperature clinozoisite+albitic plagioclase is replaced by clinozoisite+scapolite and then by scapolite+anorthitic plagioclase. Muscovite is replaced by K-feldspar with increasing temperature, whereas biotite is replaced by clinopyroxene. The pseudosection does not involve amphibole or garnet, the chosen bulk rock composition not allowing these minerals to be stable at the given conditions.

Calculated buffering paths indicate how the mineral content of the calc-schists evolve with increasing temperature. A closed system („balloon") model was used in the calculation of four buffering paths starting at four different mineralogical compositions. They all have in common the increase of X_{CO2} of the fluid phase with increasing temperature. The evolution within trivariant fields contributes considerably to this enrichment, whereas the evolution within higher variance fields tends to be less important with respect to CO_2 enrichment, given the different buffering capacities of the assemblages. Although the closed system assumption is very restrictive – the rocks may have lost fluid by devolatilisation during their evolution – the calculated paths are likely to give an indication of the minimal X_{CO2} increase. Allowing fluid loss, the X_{CO2} increase would be larger, with further passage in the trivariant fields and flatter paths within higher variance fields. This increase would be lessened if H_2O-rich fluids were infiltrating the calc-schists from the surrounding metapelitic sediments during the heating event. As the influential trivariant fields are more or less isothermal for larger X_{CO2}, the exact buffering paths have little effect on the temperature of appearance of new minerals with increasing temperature.

The starting assemblage clinozoisite–Na-rich plagioclase (plc)–muscovite–biotite causes clino-

Table 6 Average of 9 whole-rock chemical analyses of calc-schist with minimum and maximum values given. * H_2O is calculated from LOI and CO_2, which was determined by coulometric titration.

	average	min value	max value
SiO_2	44.64	36.62	54.48
TiO_2	0.41	0.27	0.63
Al_2O_3	9.43	5.77	14.80
Cr_2O_3	0.01	0.00	0.02
Fe_2O_3	3.45	2.26	5.80
MnO	0.10	0.04	0.15
MgO	2.31	1.31	5.53
CaO	21.74	13.45	27.94
Na_2O	0.57	0.42	0.82
K_2O	1.53	0.56	2.60
P_2O_5	0.15	0.08	0.60
CO_2	14.02	4.98	21.62
H_2O*	0.11	< 0.10	0.51
Total	98.47		

a) Outer part

	⑥ Val Blenio			④ Campolungo			⑤ Valle Maggia			⑦ Gondo			⑪ Val Formazza		
	P,T ↗	max.	P,T ↘	P,T ↗	max.	P,T ↘	P,T ↗	max.	P,T ↘	P,T ↗	max.	P,T ↘	P,T ↗	max.	P,T ↘
sc															
pl															
ksp															
q															
cz															
cc															
dol															
bi															
mu															
chl															
di															
hbl															
grt															

b) Middle part

	③ Cima Lunga			⑧ Crèvola d'Ossola			⑨ Val Cairasca			⑩ Alpe Dèvero		
	P,T ↗	max.	P,T ↘	P,T ↗	max.	P,T ↘	P,T ↗	max.	P,T ↘	P,T ↗	max.	P,T ↘
sc												
pl												
ksp												
q												
cz												
cc												
dol												
bi												
mu												
chl												
di												
hbl												
grt												

c) Central part

	① Gesero			② Castione		
	P,T ↗	max.	P,T ↘	P,T ↗	max.	P,T ↘
sc						
pl						
ksp						
q						
cz						
cc						
dol						
bi						
mu						
chl						
di						
hbl						
grt						

Fig. 8 Mineral assemblages and mineral evolution in calc-schists from the Central Alps. (a) Outer part: lower amphibolite facies conditions, (b) middle part: intermediate amphibolite facies conditions, (c) central part: upper amphibolite facies conditions.

pyroxene to form as the first (path 1, Fig. 9) or the second new phase (path 2, Fig. 9). The next phase appearing is K-feldspar while muscovite disappears. Finally biotite becomes unstable. Starting with the assemblage clinozoisite–Na-rich plagioclase (plc)–chlorite–muscovite (path 3, Fig. 9) the first new phase to form is scapolite followed by biotite while clinozoisite and later plagioclase (plc) is consumed. With increasing temperature a new Ca-rich plagioclase (pli) forms before chlorite is finally consumed. After the formation of K-

feldspar, muscovite vanishes. Clinopyroxene is the last phase to form before biotite disappears. Buffering path calculations for the assemblage scapolite–Na-rich plagioclase (plc)–chlorite–muscovite (path 4, Fig. 9) show that biotite and then dolomite form before the Na-rich plagioclase (plc) vanishes. Dolomite is consumed before Ca-rich plagioclase forms and reappears again with increasing temperature and X_{CO_2}. Chlorite disappears before the final disappearance of dolomite. At higher temperature the assemblage evolution
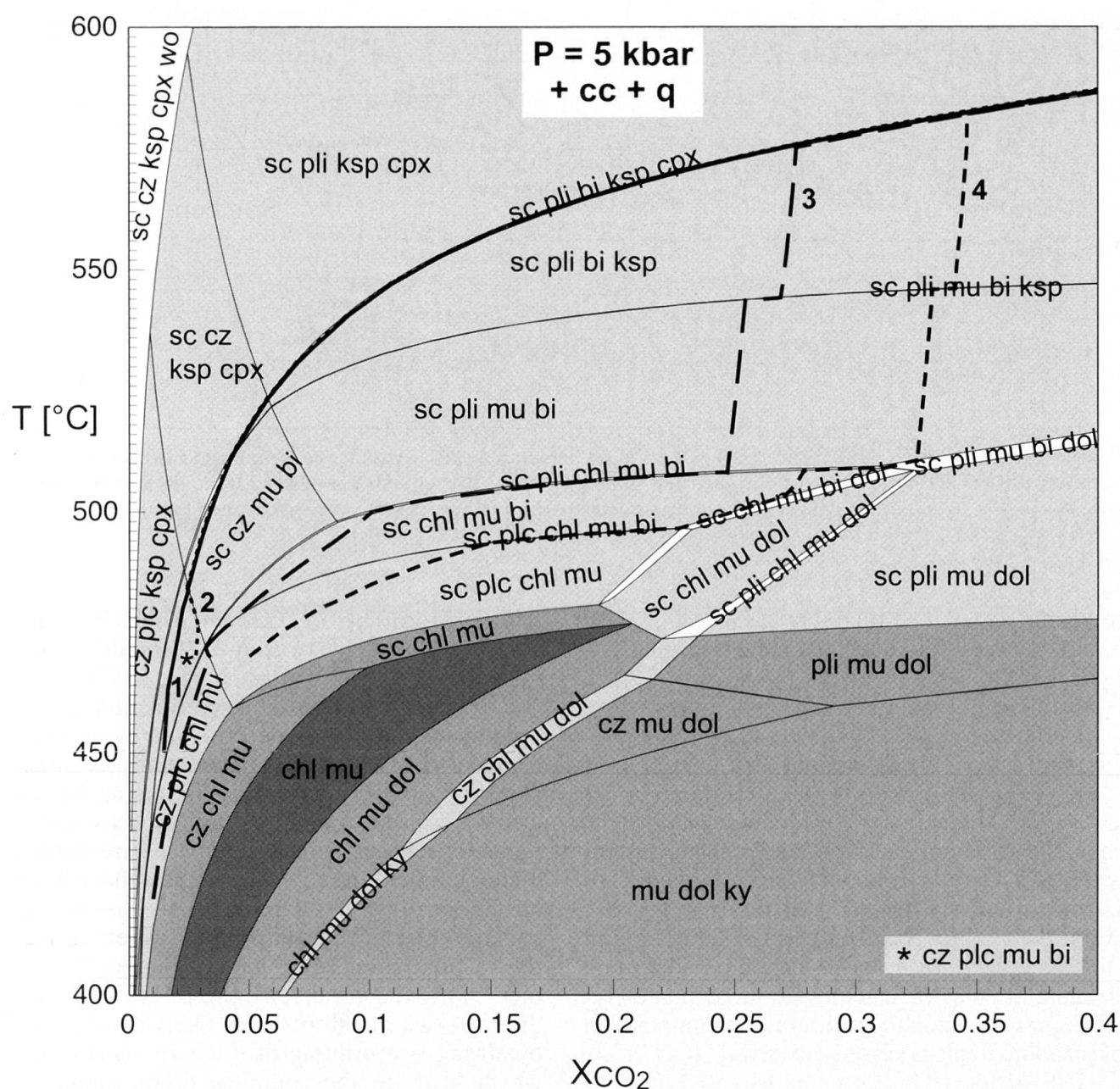

Fig. 9 T–X_{CO_2}-pseudosection at 5 kbar calculated for the average calc-schist composition given in Table 6. Stable mineral assemblages of different variance are shaded in different grey tones (Variance = 6: dark grey; 5: grey; 4: light grey; 3: white). Trivariant fields are often extremely thin, so that they appear as lines. They are labelled by 5-phase assemblages. Calculated buffering paths for four different starting compositions (1: cz-plc-mu-bi at T = 450 °C, X(CO2) = 0.014, 2: cz-plc-mu-bi at T = 470 °C, X(CO2) = 0.028, 3: cz-plc-chl-mu at T = 420 °C, X(CO2) = 0.01, 4: sc-cz-chl-mu at T = 470 °C, X(CO2) = 0.05).
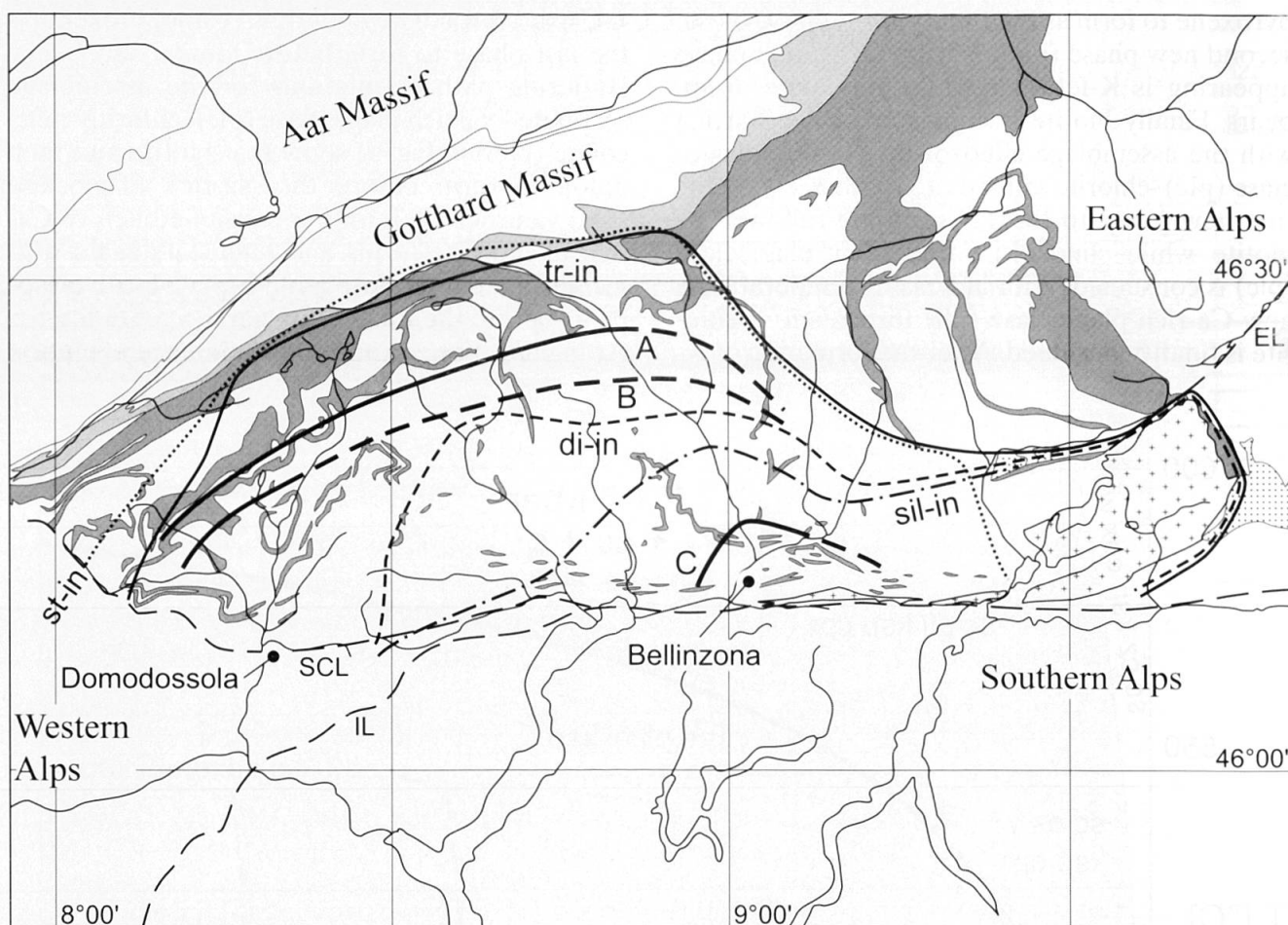
Fig. 10 Schematic map of the Central Alps from Fig. 1 showing the approximate geographic location of the transition clinozoisite+plagioclase to scapolite-bearing assemblages (*A*), the appearance of K-feldspar (*B*) and the appearance of clinopyroxene (*C*) in calc-schists, superimposed on the Geological map of Switzerland (1980).

following path 4 is comparable to the one of path 3 (Fig. 9) except that the coexisting fluid phase is richer in CO_2.

7. Discussion

The mineral assemblages observed in calc-schists show the succession, clinozoisite to plagioclase to scapolite (+ cc + q + mu + bi) from the outer towards the inner part of the Central Alps (Fig. 10). Additionally the occurrence of K-feldspar and clinopyroxene together with scapolite is observed, defining the mineral assemblage succession of Table 5. In thin section the retrograde decomposition of scapolite to plagioclase is observed.

The calculated buffering paths 1 to 3 of Fig. 9 indicate that, starting with a clinozoisite–Na-rich plagioclase assemblage, scapolite is one of the first phases to form with increasing temperature. This is in good agreement with the observations made in the calc-schists. Starting with cz + plc + mu + bi (path 1 or 2, Fig. 9) clinopyroxene and K-

feldspar form before Ca-rich plagioclase. This contradicts the observation of scapolite coexisting with Ca-rich plagioclase before K-feldspar or clinopyroxene are present. Therefore neither path 1 nor path 2 explains the observed evolution of the calc-schists. Assuming the starting assemblage is cz + plc + chl + mu (path 3, Fig. 9) scapolite followed by biotite and Ca-rich plagioclase appear before K-feldspar and clinopyroxene are stable at higher temperatures. Besides the fact that chlorite has not been observed in the starting assemblage – all the chlorite being interpreted as retrograde – the calculated buffering path 3 is in good agreement with the observed assemblage evolution. The absence of chlorite may likely be explained by strong overprinting of the early assemblages which leads to the complete disappearance of chlorite. If the Alpine calc-schists evolved along such a buffering path, it would mean that in the middle and the central part of the Central Alps plagioclase belongs to the stable assemblage at peak metamorphic conditions for this bulk-rock composition.

The regional distribution of the observed mineral assemblages allows the definition of characteristic mineral zones in the calc-schists of the Central Alps which are separated by isograds defining the appearance of a new characteristic mineral (e.g. scapolite, K-feldspar, clinopyroxene) within the mineral assemblage (Fig. 10):

The outermost zone is characterised by the presence of plagioclase and/or clinozoisite and by the absence of scapolite.

In a second zone scapolite is stable. The appearance of scapolite (isograd *A* in Fig. 10) can be explained by the reactions (see section 4):

(1) cc + 3 pl = sc
(2) 2 cz + CO_2 = sc + H_2O
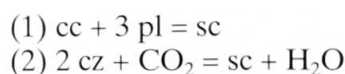
In the third zone scapolite coexists with K-feldspar. For the appearance of K-feldspar (isograd *B* in Fig. 10) several reactions can be formulated, an important being the quartz-muscovite consuming one:

(3) 2 q + sc + mu = ksp + 4 pl + H_2O + CO_2

In the innermost zone additionally clinopyroxene is stable (isograd *C* in Fig. 10). A possible reaction in the system NCKFMASCH being:

(4) 3 cc + 6 q + bi = 3 cpx + ksp + H_2O + 3 CO_2

During this study the distinction between the zones where scapolite or scapolite+K-feldspar is stable, has not been observed directly in thin section, although it is clear in the pseudosection (Fig. 9). Additionally, the investigation of calc-schist along a cross-section in Val Cairasca by Frank (1983) shows clearly the geographical separation between the „sc-in“ and „mu-cc-q-out“ isograds (Fig. 27 of Frank, 1983), the latter being comparable with the appearance of K-feldspar at isograd *B*.

A further point of discussion is the meaning of the three distinct plagioclase composition ranges found (Fig. 6), also observed along the scapolite-plagioclase grain boundary in Fig. 7. With reference to the latter, plagioclase 1 and scapolite represent the stable assemblage at peak metamorphic conditions, as most of the plagioclase surrounding the scapolite in the presence of calcite is anorthite-rich. The slightly more Na-rich plagioclase (2) forming a rim towards scapolite appears to represent a re-equilibration of plagioclase in the presence of scapolite, but most likely in the absence of calcite. The most albitic plagioclase (3), proximal to the scapolite and coexisting with cal-

cite, is interpreted to be the product of a retrograde breakdown of scapolite to plagioclase and calcite. Plagioclase that shows irregularly shaped Na-rich rims in calcite-bearing assemblages may reflect the attempted diffusive equilibration of plagioclase with scapolite under retrograde conditions when the plagioclase composition in the plagioclase–scapolite–calcite assemblage is albitic, as seen directly in (3) in Fig. 7.

8. Conclusions

Calc-schists show a succession of characteristic mineral assemblages with increasing metamorphic grade which correspond well with the stable mineral assemblages predicted by the phase diagram (Fig. 9). The first appearance of scapolite indicates a minimum temperature of 460 °C at an assumed pressure of 5 kbar (isograd *A* in Fig. 10). The appearance of K-feldspar in the absence of clinozoisite (isograd *B* in Fig. 10) indicates a minimum temperature of 520 °C (at 5 kbar). Clinopyroxene in the absence of clinozoisite (isograd *C* in Fig. 10) indicates a minimum temperature of 525 °C (at 5 kbar). However, for the suggested buffering path 3 a temperature of > 570 °C is more likely. The regional distribution of these newly defined isograds in calc-schists together with the classical isograds (Niggli and Niggli, 1965; Trommsdorff, 1966; Wenk, 1962) depicts the increasing grade of metamorphism in the Central Alps from the outer part towards the region of Bellinzona (Gesero). Although it is clear that temperature increases from the outer to the central part of the Central Alps, the way the pressure changes is not well constrained. The new isograds all move up temperature with increasing pressure by about 30 °C per kbar (Kuhn and Powell, in prep.). At the high-grade end, the presence of sillimanite and not kyanite during anatexis indicates a maximum pressure of about 7 kbar at 650 °C (via the wet solidus of metapelites).

These results are in good agreement with the current knowledge about metamorphism in the Central Alps (Frey et al., 1974; Niggli and Niggli, 1965; Todd and Engi, 1997; Trommsdorff, 1966; Wenk, 1970), also providing a validation of the new thermodynamic model for scapolite.

References

Baker, J. and Newton, R.C. (1994): Standard thermodynamic properties of meionite, $Ca_4Al_6Si_6O_{24}CO_3$, from experimental phase equilibria data. *Am. Mineral.* **79**, 478–484.

Bianconi, F. (1971): Geologia e petrografia della regione del Campolungo. *Beitr. Geol. Karte Schweiz* 142, 237.

Blattner, P. (1965): Ein anatektisches Gneissmassiv zwischen Valle Bodengo und Valle Livo (Prov. Sondrio und Como). *Schweiz. Mineral. Petrogr. Mitt.* **45**, 973–1072.

Burckhardt, C.E. (1942): Geologie und Petrographie des Basodino-Gebietes (nordwestliches Tessin). *Schweiz. Mineral. Petrogr. Mitt.* **22**, 99–186.

Burri, T., Berger, A. and Engi, M. (2005): Tertiary migmatites in the Central Alps: Regional distribution, field relation, conditions of formation, and tectonic implications. *Schweiz. Mineral. Petrogr. Mitt.* **85**, 215–232.

Ellis, D.E. (1978): Stability and phase equilibria of chloride and carbonate bearing scapolites at 750 °C and 4000 bar. *Geochim. Cosmochim. Acta* **42**, 1271–1281.

Fox, J.S. (1975): Three-dimensional isograds from the Lukmanier Pass, Switzerland, and their tectonic significance. *Geol. Magazine* 112, 547–564.

Frank, E. (1983): Alpine metamorphism of calcareous rocks along a cross-section in the Central Alps: occurence and breakdown of muscovite, margarite and paragonite. *Schweiz. Mineral. Petrogr. Mitt.* **63**, 37–93.

Frey, M. (1974): Alpine metamorphism of pelitic and marly rocks of the Central Alps. *Schweiz. Mineral. Petrogr. Mitt.* **54**, 489–506.

Frey, M. (1978): Progressive low-grade metamorphism of a black shale formation, Central Alps, with special reference to pyrophyllite and margarite bearing assemblages. *J. Petrology* **19**, 95–135.

Frey, M., Hunziker, J.C., Frank, W., Bocquet, J., Dal Piaz, G.V., Jäger, E. and Niggli, E. (1974): Alpine metamorphism of the Alps: a review. *Schweiz. Mineral. Petrogr. Mitt.* **54**, 247–290.

Geologische Karte der Schweiz (1980): 2. ed. 1:500'000. Schweizerische Geologische Kommission.

Goldsmith, J.R. and Newton, R.C. (1977): Scapolite-plagioclase stability at high pressures and temperatures in the system $NaAlSi_3O_8$-$CaAl_2Si_2O_8$-$CaCO_3$-$CaSO_4$. *Am. Mineral.* **62**, 1063–1081.

Günthert, A. (1954): Beiträge zur Petrographie und Geologie des Maggia-Lappens (NW Tessin). *Schweiz. Mineral. Petrogr. Mitt.* **34**, 1–159.

Holland, T. and Powell, R. (1998): An internally consistent thermodynamic data set for phases of petrological interest. *J. Metamorphic Geology* **16**, 309–343.

Klaper, E.M. (1982): Deformation und Metamorphose in der nördlichen Maggia-Zone. *Schweiz. Mineral. Petrogr. Mitt.* **62**, 47–76.

Klaper, E.M. (1986): Deformation und Metamorphose im Gebiet des Nufenenpasses, Lepontinische Alpen. *Schweiz. Mineral. Petrogr. Mitt.* **66**, 115–128.

Klaper, E.M. and Bucher-Nurminen, K. (1987): Alpine metamorphism of pelitic schists in the Nufenen Pass area, Lepontine Alps. *J. Metamorphic Geology* **5**, 175–194.

Knoblauch, P. and Reinhard, M. (1939): Erläuterungen zum Geologischen Atlas der Schweiz, 1:25000, Blatt San Jorio. Schweiz. Geol. Kommission.

Kuhn, B.K. (2005): Scapolite stability: Phase relations and chemistry of impure metacarbonate rocks in the Central Alps. Unpubl. PhD, ETH Zürich, 127 pp.

Moecher, D.P. and Essene, E.J. (1990): Phase equilibria for calcic scapolite, and implications of variable Al–Si disorder for P–T, T–X_{CO2}, and a–X relations. *J. Petrology* **31**, 997–1024.

Niggli, E. (1960): Mineralzonen der alpinen Metamorphose in den Schweizer Alpen.: International Geological Congress XXI Session Norden. Part B. Copenhagen, 132–135.

Niggli, E. and Niggli, C.R. (1965): Karten der Verbreitung einiger Mineralien der alpidischen Metamorphose in den Schweizer Alpen (Stilpnomelan, Alkali-Amphibol, Chloritoid, Staurolith, Disthen, Sillimanit). *Eclogae geologicae Helveticae* **58**, 335–368.

Niggli, P., Preiswerk, H., Grütter, O., Bossard, L. and Kündig, E. (1936): Geologische Beschreibung der Tessiner Alpen zwischen Maggia- und Bleniotal. *Beitr. Geol. Karte Schweiz* **71**, 190 pp.

Oterdoom, W.H. (1979): Plagioclas-scapolite-calcite phase relations in High metamorphic argillaceous limestones. *Schweiz. Mineral. Petrogr. Mitt.* **59**, 417–422.

Oterdoom, W.H. (1980): Scapolite in metamorphic calc-silicate rocks: Crystallographic and phase relations. Unpubl. PhD, ETH Zürich, 134 pp.

Oterdoom, W.H. and Gunter, W.D. (1983): Activity models for plagioclase and CO_3–scapolite – an analysis of field and laboratory data. *Am. J. Science* **283-A**, 255–282.

Powell, R., Holland, T. and Worley, B. (1998): Calculating phase diagrams involving solid solutions via non-linear equations, with examples using THERMOCALC. *J. Metamorphic Geology* **16**, 577–588.

Todd, C.S. and Engi, M. (1997): Metamorphic field gradients in the Central Alps. *J. Metamorphic Geology* **15**, 513–530.

Trommsdorff, V. (1966): Progressive Metamorphose kieseliger Karbonatgesteine in den Zentralalpen zwischen Bernina und Simplon. *Schweiz. Mineral. Petrogr. Mitt.* **46**, 431–460.

Trommsdorff, V. (1990): Metamorphism and tectonics in the Central Alps: The Alpine lithospheric mélange of Cima Lunga and Adula. *Memorie della Società geologica Italiana* **45**, 39–49.

Wenk, E. (1962): Plagioklas als Indexmineral in den Zentralalpen. Die Paragenese Calcit-Plagioklas. *Schweiz. Mineral. Petrogr. Mitt.* **42**, 139–152.

Wenk, E. (1970): Zur Regionalmetamorphose und Ultrametamorphose im Lepontin. *Fortschritte der Mineralogie* **47**, 34–51.